Improvement of Motion Estimation of the Taku Glacier using Spaceborne SAR Images

LI FANG [1], OLIVER MAKSYMIUK [1], MICHAEL SCHMITT [1] & UWE STILLA [1]

In dieser Arbeit wird die Oberflächengeschwindigkeit des Taku Gletschers (Juneau, Alaska) mit einem Korrelationsansatz aus hoch aufgelösten TerraSAR-X Daten mehrerer Überflüge geschätzt. Die Genauigkeit liegt dabei im Bereich von 2 cm/Tag mit einer hohen Zuverlässigkeit. Letztere wird durch einen Vergleich zwischen dem Maximum der Korrelation und seiner gemittelten Nachbarschaft bestimmt. Um die Zuverlässigkeit und die Abdeckung weiter zu erhöhen wird in dieser Arbeit eine Markov Zufallsfeld (MRF) verwendet, um die Daten eines aufsteigenden und abfallenden Orbits zusammenzuführen. Das Verfahren hilft an Stellen, die durch Schatten oder andere Artefakte keine zuverlässigen Messungen erlauben, eine Schätzung der Geschwindigkeit durchzuführen. Des Weiteren wird die Genauigkeit im Gesamten verbessert, da redundante Informationen konsequent genutzt und Widersprüche durch das Modell aufgelöst werden.

1 Introduction

The outlet glaciers of ice sheets, the main means of transporting ice from the interior to the oceans, play a very important role in the research of ice sheet variations, due to their flow velocity as one control parameter determining the mass balance. Especially, for small icefields, the mass-loss recently has become an excellent cryosphere contributor to sea level changes.

Even if in situ observations (e.g., GPS) of glacier motion can be of high accuracy level, they are costly and limited at the spatial coverage compared with remote-sensing data. The satellite remote-sensing data acquired from several sensors can help in those cases. Satellite optical imagery data have been examined to be useful sources as they provide visible features for the tracking procedure (SCAMBOS et al., 1992). However, the method relies on illumination by the sun, resulted in their dependence on weather conditions which cannot provide timely information of the target area. In contrast, SAR, an active microwave remote-sensing instrument, can obtain timely data with a spatial resolution compatible with the topographic variation by emitting its own energy, providing the ability to measure centimeter scale changes on the Earth's surface (HØGDA et al., 2010).

Much work has been successfully done to map glacier velocities by radar imagery using the feature tracking method, a cross-correlation based technique, for fast-moving ice (i.e. outlet glaciers), when interferometry and coherence tracking methods are ineffective because of the loss of phase coherence and large displacements (STROZZI et al., 2002; DE LANGE et al., 2007).

---

1) Photogrammetrie & Fernerkundung, Technische Universität München (TUM),
Arcisstraße 21, 80333 München, http://www.pf.bv.tum.de

Some research work has reported that the accuracy of ice velocity estimation using the intensity tracking technique can be on the order of 2cm/d when applied on high resolution repeat pass TerraSAR-X data with 11 days interval (FLORICIOIU et al., 2008; FLORICIOIU et al., 2009; EINEDER et al., 2011).
However, often, the cross-correlation technique does not find matches of features in "data holes" in the SAR scenes affected by radar shadowing and specular backscattering of smooth ice surface, and therefore fails to derive the surface velocities of glaciers in mountainous areas. For this case, this paper proposes a fusion of velocity maps at same region and acquisition time derived from the two different imaging geometries from ascending and descending satellite tracks, aiming to reduce the effects of data holes on ice motion estimation.

2 SAR Data Preprocessing

The Juneau Icefield is a low-latitude glacier system of small scale located in southeast Alaska, with the Taku Glacier as its principal outlet glacier. Current researches in Taku Glacier suggest that ice fluxes have been nearly stable for a long period (MCGEE et al., 2007; PELTO et al., 2008). In this paper, the scenes of Taku Glacier imaged by high resolution TerraSAR-X are applied for experiments. All the experimental works in this paper are based on TerraSAR-X repeat cycle data acquired in stripmap mode from two different imaging geometries (ascending and descending) between end of June and early August 2009 (see Table 1).

Table 1. TerraSAR-X data delineation used for ice motion estimation (SM-stripmap mode).

Imaging Mode	Acquisition Time	Incidence Angle Min	Incidence Angle Max	Pass Direction	Orbit
SM	2009-06-30T02:31:42	33,77	36,93	ascending	137
SM	2009-06-30T15:27:06	26,95	30,57	descending	145
SM	2009-07-11T02:31:42	35,81	38,79	ascending	137
SM	2009-07-22T02:31:43	35,80	38,79	ascending	137
SM	2009-08-02T02:31:44	33,77	36,93	ascending	137
SM	2009-08-02T15:27:08	26,94	30,57	descending	145

The TerraSAR-X Single Look Slant Range Complex (SSC) data were operationally processed into the geo-coded data using a precise available DEM (courtesy of the Chair of Geodesy, TU München). The enhanced data have a ground resolution of 3m with pixel spacing of 1.5 m in both azimuth and range direction. The geo-coded SAR scenes used in this paper are plotted on the ground truth area shown in Fig.1.

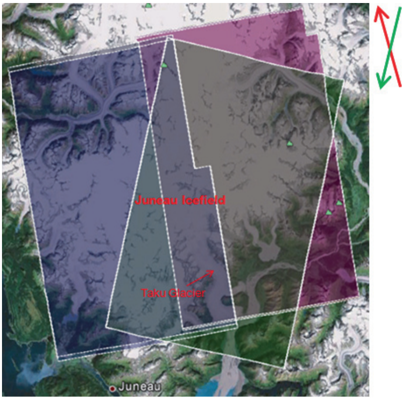

Fig. 1. Ground coverage of geo-coded SAR data plotted on an optical image of the scene. Red arrow: azimuth direction of ascending orbit; Green arrow: azimuth direction of descending orbit. In both tracks, TerraSAR-X is right looking. (Underlying optical image ©2012 Google Earth)

3 Offset Tracking

3.1 Cross-Correlation Technique

The feature tracking technique, which has been described in detail in (Strozzi et al., 2002; de Lange et al., 2007), was applied on the high resolution geo-coded ground range TerraSAR-X images to generate two dimensional velocity maps. The offset maps are generated by seeking the peak in the normalized cross correlation field obtained by patches from two sequential SAR intensity imageries. The successful estimation of offsets relies on the identical glacier surface features (e.g., crevasses or drainage patterns) at the scale of patches used. According to the coarse information about the velocity rate of Taku Glacier, we assumed that the maximal displacement between two successive images, with 11days cycle, is 22 meters (about 15 pixels) on the ground. Then, the sizes of sample widow and search window employed in this work are in the order of 216x216 and 296x296 pixels which are enough for the assumed displacements. In order to achieve sub-pixel accuracy, around the correlation peak, a two dimensional regression fit is employed around the correlation peak in order to obtain the newly modeled correlation peak, which is used to replace the original one, by a window (5x5 pixels). A correlation signal-to-noise ratio (SNR) expressing the comparison of the modeled correlation peak relative to the remained average value of the original correlation field is employed as confidence measurement.

3.2 Error Analysis

The absolute error of the glacier motion estimation can be calculated using the cross-correlation method for individual patches from the zero-velocity zones (i.e. rock areas) in SAR scenes. In this paper, the absolute error is computed by dividing the averaged offsets of several individual patches from stable zones located in different parts of the scene by the observation cycle.

3.3 Tracking Results

Since we perform the technique described above on the geo-coded SAR intensity images, the region of interest (ROI) – the Taku Glacier – is extracted from every scene using the geometric annotation information available in the metadata. The 2D velocity vector maps, at the same region and acquisition time, are generated using images from ascending and descending satellite tracks separately.

The calculated absolute error in this paper, using the method above, is 0.032m/d, sufficient for the ice motion estimation, which is lightly smaller than 0.036m/d in (FLORICIOIU et al., 2009). The raw result of the estimated motion map with 11.37 as the averaged SNR value, and velocities with high correlation confidence level from ascending and descending tracks are shown in Fig.2, separately.

Note that for this illustration, the outliers were culled out first by applying various rejection criteria, for instance an SNR value of 6 as lower threshold, neighborhood motion values, or flux direction.

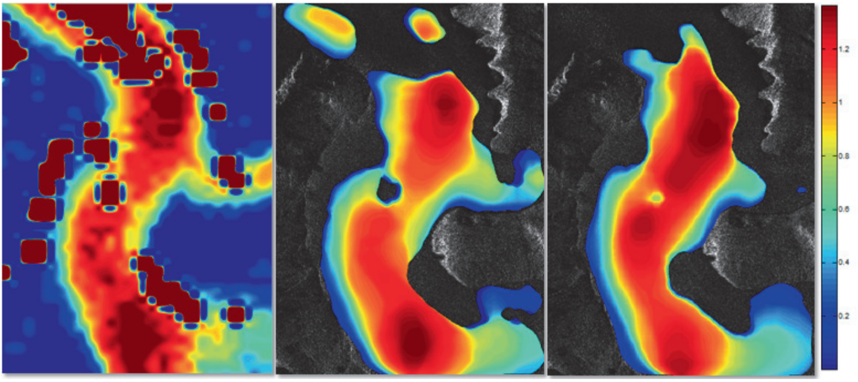

Fig. 2. Motion maps from the surging area of Taku Glacier. Left: Raw motion map. Middle: Motion map from ascending data after culling outliers. Right: Motion map from descending data after culling outliers.

It was found that some estimated data holes caused by radar shadowing that are found in the motion map derived from the ascending SAR data are successfully filled with information from the descending data with reliable SNR values. That is also true when reversely applied. Additionally, there are some holes located at the same area in motion maps derived from both satellite tracks. This should be due to the lack of features in some ice areas caused by specular backscattering due to the smooth ice surface that acts like a mirror. Thus, fusing the motion maps derived from the two different imaging geometries can help to reduce the 'data holes' and improve estimation accuracy by redundant measurements.

4 Fusion Procedures

The fusion of estimated velocities from different satellite tracks has two main concerns. The first is to enlarge the coverage area of estimation results for the scene and the second is to improve the estimation accuracy.

4.1 Weighted Averaging

The simplest method to fuse estimated motion maps from different imaging geometries is the weighted average method. In Fig.4, on the left side, the fused ground 2D velocity maps using raw motion maps from both satellite geometries by applying the weighted average method using the related SNR value as weight is shown. Obviously, this fusion result is not reliable because of the sharp edge of motion values in the glacier body. Then, we try to find another fusion method to generate more reasonable results.

4.2 Markov Random Field

The other problem concerns the estimated velocities where the measurements or estimations from a single track are contradictory to each other. If both estimations have almost the same SNR the most simple solution to fuse the tracks, namely weighted averaging, would not work. In this case it is advantageous to use local context to resolve the contradictions. We propose Probabilistic Graphical Models (PGM), more specific a Markov Random Field (MRF), as a framework for the fusion. The flexibility of PGMs to model the domain allows to benefit from the contradictions and redundant measurements. Additionally it is possible to impose some further model knowledge. One evident constraint is the smoothness of the surface velocity. It is very unlikely that a discontinuity appears in just a few measurements. The domain model used in this work is shown in Fig. 3.

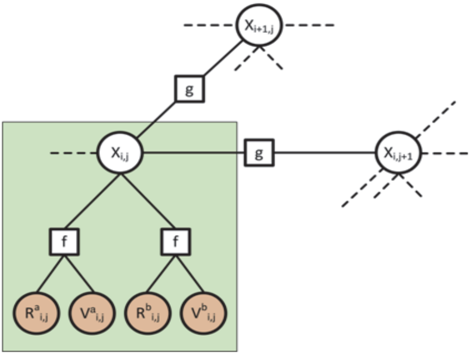

Fig. 3. Structure of the PGM used for the fusion of multiple tracks. The observations (red) are connected to the variables representing the estimated state of the surface velocity. These variables themselves are connected in a grid to impose a smoothness constraint.

The variable $X_{i,j}$ represent the discretized surface velocity of the glacier at discrete position (i, j) and are the true state which is subject to estimation. Variables $R^{x}_{i,j}$ and $V^{x}_{i,j}$ are the observations namely the SNR and the estimated velocity from track x. The model for posterior distribution, after (LI, 2009), is given as

$$P(X \mid R,V) = \frac{1}{Z}[P(R,V \mid X)P(X)] \tag{1}$$

Our state variables set X is connected to the observations by factors and represents the "data term" of the network. These factors connect three different entities with the following relationship

$$P(R,V \mid X) = \frac{1}{\sqrt{2\pi\sigma_1^2}} \exp^{-\frac{(X-V)^2}{2\sigma_1^2}} \tag{2}$$

where factor σ_1 expresses the strength of σ_0 relative to the SNR.

The interaction between the variables in a PGM can be interpreted as probabilities or as energies. Despite the interpretation the optimization tries to find an extremum for the joint assignment of all variables in the network. We use a Gaussian likelihood to model the relationship between the variable and its observations. Therefore we use the causal model that the true state causes the appearance of the pixels in the different tracks. Furthermore, the model implies a conditional independence of the pixels of the tracks given the true state X. As can be seen in (2) we consider the SNR as a reliability measure for the single measurements. The higher the SNR, the more reliable the corresponding measurement and the smaller the variance will be. As a consequence the factor is much more restrictive in the deviation of the true state from the observation if the SNR is high. It should be noted that the model can be used with any number of tracks.

The other kind of factors is used to define the "smoothness term" and allows imposing some regularization to the state variables. They are particular useful in the aforementioned case of contradictory observations. In this case the regularization resolves the contradiction by using local context to determine the best state. The smoothness factors are defined by

$$P(X) = \prod_{i} \prod_{j \in N_i} p(X_i, X_j) \tag{3}$$

$$P(X) = \frac{1}{\sqrt{2\pi\sigma_2^2}} \exp^{-\frac{(X_i - X_j)^2}{2\sigma_2^2}} \tag{4}$$

where X_j are the 8 neighbor pixels of X_i.

It should be noted that PGMs are not the only approach to implement this kind of model. There are even analytical methods to obtain a solution for this problem. One advantage is the flexibility of the PGMs to model almost any kind of dependency. To improve the fusion we allow discontinuities in the model. This results in a smoother velocity distribution and leads to more accurate boundaries of the glacier. To adapt the model we have to use bounded functions, deduced from equations (2) and (4), which now are defined by

$$P(R,V \mid X) = \frac{1}{\sqrt{2\pi\sigma_1^2}} \exp^{-\frac{[\min(|X-V|,\beta)]^2}{2\sigma_1^2}} \tag{5}$$

$$P(X) = \frac{1}{\sqrt{2\pi\sigma_2^2}} \exp^{-\frac{[\min(|X_i - X_j|,\gamma)]^2}{2\sigma_2^2}} \tag{6}$$

where factor β is the threshold for the maximum difference between state X and the observation value, and, also, γ is the threshold for the maximum difference between state X_i and neighbor pixels X_j. σ_0, β, σ_2 and γ are input parameters in this graphical model, and, considering the physic of glacier flow, we set these parameters as 30, 1.5, 5, 0.2 separately. The overall solution is obtained by running inference (loopy belief propagation) on the resulting graph.

The fusion result using raw motion maps from ascending and descending tracks, by applying the above graphical model, is plotted on the right side of Fig. 4, which is smoother in velocity distribution and reasonable concerning the physics of glacier flow.

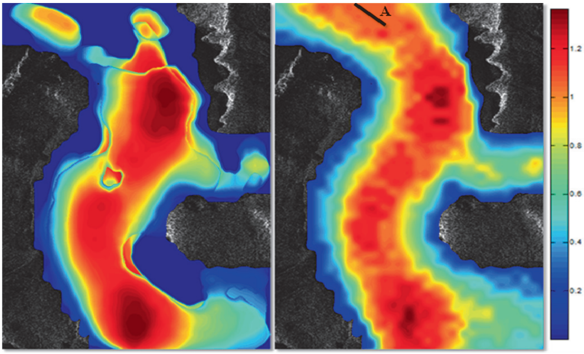

Fig. 4. Motion maps after fusion of estimation results from ascending and descending satellite tracks. Left: Fusion result using weighted average. Right: Fusion result using PGM.

4.3 Glacier Motion Result

The velocity pattern on Taku Glacier agrees well with the ground GPS observation exploited by the Juneau Icefield Research Program (JIRP). As the ice fluxes have been nearly stable for a long period, we can compare the estimated result with recent ground GPS observations. In the right graph of Fig. 4., along the center line A (black) located in upper part of the examined glacier body, the average velocity value is 1.09m/d and with the maximum value at the lowest part of line A as 1.107m/d which is slightly lower than that of 1.14m/d by ground survey in (MCGEE et al., 2001), possibly due to the absolute error 0.032m/d calculated in this paper.

5 Conclusion and Recommendations

The study on the outlet area of the Taku Glacier demonstrates the remarkable capabilities of TerraSAR-X stripmap mode data for deriving ice motion maps by a using cross correlation based technique. However, due to the “data holes” in the SAR scenes affected by radar shadowing and backscattering properties, especially in mountainous areas, the feature tracking method fails to derive the surface velocities of glaciers in those areas. In this case, fusion of motion maps deduced from both satellite imaging geometries can be a good solution. We have shown that the use of the weighted average method for fusion is not reliable. On the contrary, the markov random field has shown its unique capabilities on fusion of motion maps from different data sources. Additionally, fusion of motion maps can also enhance the overall accuracy by exploitation of redundant measurements. Therefore, for velocity estimation of glacier using spaceborne SAR images, the fusion of motion maps deduced from complementary orbits can greatly improve the result.

Acknowledgment

The authors would like to thank Prof. Thomas Wunderlich , Chair of Geodesy, Technische Universität München (TUM) and Dr. Oliver Lang of Infoterra GmbH / Astrium GeoInformation Services for providing the data used in this study.

6 References

DE LANGE, R.; LUCKMAN, A. & MURRAY, T., 2007: Improvement of satellite radar feature tracking for ice velocity derivation by spatial frequency filtering. IEEE Transactions on Geoscience and Remote Sensing, vol. 45, no. 7, pp. 2309-2318.

EINEDER, M.; ABDEL-JABER, W.; FLORICIOIU, D.; ROTT, H. & YAGUE-MARTINEZ, N., 2011: Glacier flow and topography measurements with TerraSAR-X and TanDEM-X. IEEE International Geoscience and Remote Sensing Symposium (IGARSS).

FLORICIOIU, D.; EINEDER, M.; ROTT, H. & NAGLER, T., 2008: Velocities of major outlet glaciers of the Patagonia Icefield observed by TerraSAR-X. IEEE International Geoscience and Remote Sensing Symposium (IGARSS).

FLORICIOIU, D.; EINEDER, M.; ROTT, H.; YAGÜE-MARTINEZ, N. & NAGLER, T., 2009: Surface velocity and variations of outlet glaciers of the Patagonia icefields by means of TerraSAR-X. IEEE International Geoscience and Remote Sensing Symposium (IGARSS).

HØGDA, K. A.; STORVOLD, R. & LAUKNES, T. R., 2010: SAR imaging of glaciers. In: P. Pellikka, and W. G. Rees (Eds). Remote Sensing of Glaciers. Taylor & Francis Group, London: 153.

Li, S. Z., 2009: Markov Random Field Modeling in Image Analysis. 3rd edn, Springer, London, pp. 15-16.

MCGEE, S. & STEMPFHUBER, W. ET AL., 2007: Surface Velocity Changes on the Taku Glacier System - 1993 to 2007. Juneau Icefield Research Program, Field Session.

MCGEE, S. ET AL., 2001: The GPS data, in GPS Science on the Juneau Icefield, Alaska. Viewed on 02 December 2012, <http://www.crevassezone.org/survey-results/surface-velocity/Longitudinal-A/Longitudinal-A.htm>.

PELTO, M. S.; MCGEE, S. R.; ADEMA, G. W.; BEEDLE, M. J.; MILLER, M. M.; SPRENKE, K. F. & LANG, M., 2008: The equilibrium flow and mass balance of the Taku Glacier, Alaska 1950-2006. The Cryosphere Discussions, vol. 2, issue. 3, pp. 275-298.

SCAMBOS, T. A.; DUTKIEWICZ, M. J.; WILSON, J. C. & BINDSCHADLER, R. A., 1992: Application of image cross-correlation to the measurement of glacier velocity using satellite image data. Remote Sens. Environ., vol. 42, no. 3, pp. 177–186.

STROZZI, T.; LUCKMAN, A.; MURRAY, T.; WEGMÜLLER, U. & WERNER, C. L., 2002: Glacier motion estimation using SAR offset-tracking procedures. IEEE Transactions on Geoscience and Remote Sensing, vol. 40, no. 11, pp. 2384-2391.